GEOMAGNETIC ACTIVITY FORECASTING: THE STATE OF THE ART

Jo Ann Joselyn
NOAA Space Environment Laboratory
Boulder, Colorado

Abstract. Short-term (days to weeks) geomagnetic forecasts are valuable for a variety of public and private sector endeavors. However, forecast skill, as measured by the success of predicting geomagnetic indices, is disappointing, especially for disturbed conditions. Possible reasons for this lack of proficiency include an incomplete understanding of the solar origins of interplanetary disturbances, insufficient observations of solar phenomena and interplanetary disturbances, and an underestimation of magnetospheric-ionospheric control of observed geomagnetic activity. Until more progress can be made on each of these problems, desirable forecasting precision is likely to remain elusive. The best opportunity for improved service to those agencies requiring advance notice of geomagnetic disturbances is "nowcasting" using real-time, near-Earth observations of the approaching solar wind.

1. INTRODUCTION

The level of disturbance of the geomagnetic field serves as a convenient proxy that characterizes the level of disturbance of the near-Earth space environment, namely, the ionosphere and magnetosphere. For example, a study addressing basic, undisturbed ionospheric behavior might begin with the collection of data on geomagnetically quiet days; in contrast, a disturbed ionosphere is virtually guaranteed on geomagnetically active days. A particular advantage of geomagnetic data is that beginning with the earliest scientific studies of geomagnetic records, the data have been characterized, or indexed, by the level of disturbance. The earliest was the C index, developed in 1906, whereby the observer rated each day as 0, 1, or 2, depending on whether the day was exceptionally quiet, moderately disturbed (the normal circumstance), or significantly disturbed [*Lincoln*, 1967]. Indexing greatly facilitates the sorting of chronological geophysical data inventories into activity bins and provides a well-defined forecast parameter that can be understood and interpreted by a diverse geophysical community. Examples of geophysical models formulated using global geomagnetic indices are the thermospheric mass spectrometer–incoherent scatter model MSIS-86 [*Hedin*, 1987] and the Magnetospheric Specification and Forecasting Model (MSFM), a particle flux specification model developed for operational use [*Bales et al.*, 1993; *Freeman et al.*, 1993].

Indices necessarily represent a selected timescale of variation. The timescales of variation in Earth's magnetic field range from geologic reversals [e.g., *Jacobs*, 1984] to subsecond micropulsations [*Lanzerotti et al.* 1990]. The longest timescales are caused by internal (geologic) processes, but shorter-term geomagnetic activity is driven by variability on the Sun and fluctuations in the solar wind; indeed, geomagnetic activity cycles have been related to decade-long solar activity cycles [e.g., *Feynman and Crooker*, 1978; *Feynman*, 1982; *Feynman and Gu*, 1986; *Legrand and Simon*, 1981]. Proxy records of geomagnetic activity (auroral sightings) were used to infer solar behavior even before the time when solar observations began [e.g., *Feynman and Silverman*, 1980, *Feynman and Fougere*, 1984]. The geomagnetic field has a diurnal variation caused by tides and currents driven by a solar-heated ionosphere [e.g., *Matsushita*, 1967]. Variations on shorter timescales are ultimately driven by solar wind–magnetosphere interactions [e.g., *Axford*, 1967], whose physics and dynamics are open topics of research.

The level of disturbance of the space environment is of more than academic interest. Such private and public endeavors as communication and navigation systems, electric power networks, geophysical exploration, spacecraft control, and scientific research campaigns [e.g., *Lanzerotti*, 1979; *Joselyn*, 1986b] are affected by geomagnetic fluctuations. Daily reports and forecasts of geomagnetic activity are routine products of the 10 Regional Warning Centers of the International URSIgram and World Days Service (IUWDS). These international centers, located in the United States of America, France, Canada, China, Japan, India, Czech Republic, Poland, Russia, and Australia, serve the scientific and user communities

Published in 1995 by the American Geophysical Union.

Reviews of Geophysics, 33, 3 / August 1995
pages 383–401
Paper number 95RG01304

within their own geographical regions; they also provide, exchange, and relay data and advice on space weather to the other centers [*Thompson et al.*, 1993]. In the U.S., the agency responsible for this work is the Space Environment Laboratory (SEL) of the National Oceanic and Atmospheric Administration (NOAA). SEL's Space Environment Services Center (SESC) works around the clock to monitor more than 1400 separate data streams, which sense solar, magnetospheric, and ionospheric parameters. When certain predetermined threshold levels are exceeded, especially geomagnetic activity indices, SESC personnel immediately take action to inform subscribers.

Since 1808, episodes of extraordinary levels of geomagnetic disturbance have been known as "storms," a term attributed to Alexander von Humboldt [*Chapman*, 1968]. Magnetic storms denote variations in Earth's magnetic field intensity which may be as large as several percent of the undisturbed value measured at the surface. The frequency of storm occurrence varies over a roughly 11-year cycle but is not necessarily synchronous with the well-known sunspot cycle. At magnetic cycle maxima, most of the days of a month (but not all) can be disturbed. However, even at cycle minima, it is unusual that a month goes by without a stormy day.

A particularly severe geomagnetic storm occurred in March 1989 [*Allen et al.*, 1989]; it was the biggest storm since 1960 and has not been equaled through 1994. Reported geophysical effects of that storm included widespread auroras; satellite anomalies; a system-wide power blackout in Quebec, Canada; and peculiar radio propagation conditions [*Cliffswallow*, 1993]. While the enormity of the sunspot group and the frequency of significant flares had led SESC forecasters to predict the possibility of geomagnetic activity, the date and severity of the storm were not accurately forecast. This lack of forecasting accuracy is unfortunately not unusual.

What is the state of the art? Verification data (comparisons of forecasts with observed indices and forecasts with observed events) for the past 7 years indicate that for 1-day forecasts, overall SESC forecast quality is better than that obtained by simple techniques such as recurrence or persistence (explained further below). However, forecast accuracy tends to decrease over the longer term (K. A. Doggett, manuscript in preparation, 1995). On an annual basis, for 2 of the past 7 years, sample climatology (the simple average of the observed parameter that is being forecast) has been more skillful than the 1-day SESC forecast. For rare events (e.g., storms), SESC capability has been disappointing (missed events and false alarms occur more often than accurate forecasts).

This paper reviews the current state of short-term (days to weeks) forecasts of diurnally averaged geomagnetic activity without the benefit of timely solar wind data. Predictions of geomagnetic activity using solar wind data near 1 AU (essentially "nowcasts") are beyond the scope of this review; however, ongoing developments in understanding how the magnetosphere extracts and processes energy from the solar wind, and the hope of acquiring data from new solar wind monitors, make such nowcasts a particularly exciting and operationally relevant endeavor. This review asks the question, "Do we now have the required knowledge and data to accurately forecast a geomagnetic storm a day or so in advance of its onset?" To answer this question, the following evidence is presented. First, the index now used to describe and predict geomagnetic activity is briefly explained. This index, particularly well suited for Earth's heavily populated middle latitudes, sums the effects of multiple geophysical current systems driven by separate physical processes. By choosing to predict this index, we have selected a formidable task. Next, we discuss the general forecasts of this index using a variety of simple methods and compare it with SESC verification results, concluding that there is room for improvement. In the following two sections we review the physical tools that SESC uses to forecast activity, and try to determine which are more robust, leading to a course of action to improve geomagnetic services.

2. MEASURES OF GEOMAGNETIC ACTIVITY

J. Bartels fashioned the K index, the geomagnetic index in widest use today, in 1932 [e.g., *Chapman and Bartels*, 1940]. An excellent review and description of the K index and related global indices is given by *Menvielle and Berthelier* [1991]. The K index is a quasi-logarithmic number between 0 and 9 that is assigned at the end of specified 3-hour periods (0000–0300, 0300–0600, etc.), by measuring the maximum deviation (in nanoteslas) of the observed field beyond expected quiet field conditions, for each of the three magnetic field vector components. The largest of the maxima is converted to a K index by using a look-up table appropriate for that particular observing site. Table 1 shows the values used for Boulder, Colorado, and Fredericksburg, Virginia. This process standardizes the data by correcting for expected geophysical biases between observing sites. By way of contrast, at College, Alaska, where the magnetic field is naturally more variable owing to the proximity of the auroral electrojet, a deviation between 0 and 20 nT is coded as a K of 0, and a deviation of 2500 nT or more is necessary to code a K of 9.

At individual stations, to combine the eight daily K indices into one number representative of overall activity for the whole day, each K is converted to an a index as shown in Table 2; the a index linearizes the quasi-logarithmic K index. Then the eight a indices are arithmetically averaged to yield a daily A index. This A index is used to define a storm and describe its

TABLE 1. Observed Range of Magnetic Fluctuations and the Corresponding *K* Index for Boulder, Colorado, and Fredericksburg, Virginia

K	*Range, nT*
0	0–4
1	5–9
2	10–19
3	20–39
4	40–69
5	70–119
6	120–199
7	200–329
8	330–499
9	≥500

severity as shown in Table 3. These categories guarantee that a minor storm includes one or more *K* of 5 or greater, that a major storm includes one or more *K* of 6 or greater, and that a severe storm includes a *K* of 7 or greater. However, these categories are arbitrary and are not universally accepted; research studies can differ significantly in their assignment of activity thresholds [*Joselyn*, 1989; *Joselyn and Tsurutani*, 1991].

K (3-hourly) and *A* (daily) indices from individual observatories can be combined to create "global" indices. The best known of these are the *Kp* (and *Ap*) indices (where the *p* denotes planet-wide averaging). Alternative global indices include the *am*, *Km*, *an*, and *as* indices and the *aa* index. These indices, which differ primarily on the basis of the number and location of the geomagnetic observatories that contribute data, are also discussed by *Menvielle and Berthelier* [1991].

Other geomagnetic indices, such as *Dst* and *AE*, were defined to characterize specific current systems within the space environment [e.g., *Rostoker*, 1972; *Mayaud*, 1980]. These indices are better suited for forecasts because the physical drivers are better isolated. However, these indices are not yet available in real time and have not been adopted for operational use. Therefore in this review the challenge of forecasting local geomagnetic *K* and *A* indices will be emphasized. Future improvements in communication networks will make it possible to acquire global observatory data in near-real time and will provide new opportunities for employing and forecasting these and other physical parameters.

TABLE 2. *K* Indices and Corresponding *a* Indices

K	*a*
0	0
1	3
2	7
3	15
4	27
5	48
6	80
7	140
8	240
9	400

TABLE 3. *K* indices and Corresponding Activity Categories

Category	*A Index Range*	*Typical K Indices*
Quiet	0–7	0, 1, 2
Unsettled	8–15	3
Active	16–29	4
Minor storm	30–49	5
Major storm	50–99	6
Severe storm	100–400	7, 8, 9

3. MEASURES OF GEOMAGNETIC FORECASTING ABILITY

Verification results presented in this section are for predictions made by the SESC of the *K* (and *A*) indices measured at Fredericksburg, Virginia. Fredericksburg is a standard U.S. Geological Survey (USGS) observatory that has been in continuous operation since 1957. Fredericksburg *K* indices are still scaled by hand, and the values are telephoned daily to the SESC. Fredericksburg *K* indices are also scaled automatically using the International Association of Geomagnetism and Aeronomy (IAGA)–approved USGS procedure [*L. Wilson*, 1987] for consistency with other automated USGS observatories; these indices are further estimated, for SESC purposes, using yet another automatic scaling procedure. The USGS Boulder vector magnetometer data are fed directly into SESC, where they are continuously displayed. The USGS Fredericksburg magnetic observatory was chosen as the SESC standard because its geomagnetic latitude (49°N) is approximately the same as Boulder's; thus geomagnetic disturbances at the two sites are of comparable amplitude. *K* indices are estimated in real time for the Boulder data, and alerts are called on the basis of those indices. However, Fredericksburg *K* indices, determined independently, are used for purposes of forecast verification.

3.1. Practical Methods of Forecasting Activity

A study of the historical levels of daily geomagnetic activity indices shows that the typical condition is quiet [e.g., *Joselyn et al.*, 1988]. Figure 1 displays the distribution function of the daily *A* index for Fredericksburg from 1967–1986. Table 4 lists the number of geomagnetically disturbed days (*Ap* of 30 or greater) for solar cycle 21, showing that storm conditions are unusual and severe storms are rare. Thus a reasonable and reliable "first-cut" forecast would be for quiet conditions. This forecast method contains little useful operational guidance but verifies well, serving as a

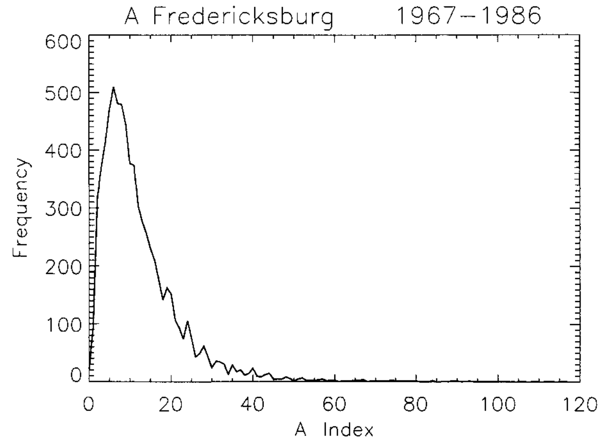

Figure 1. The *A* index is a daily measure of geomagnetic activity that ranges between 0 and 400 in units of 2 nT. The mode, or most frequently observed, geomagnetic *A* index for Fredericksburg, Virginia, between February 1966 and May 1983 was 6, which is quiet. The median index was 10.

reminder to builders of geomagnetic forecasting algorithms that they must adequately predict the norm: quiet conditions.

An improvement to a blind forecast of quiet conditions is one that includes knowledge of longer-term average conditions, or climatology. The strong semiannual periodicity in geomagnetic storm occurrence is illustrated in Figure 2. This tendency has been examined by a long list of researchers [e.g., *Bartels*, 1963; *Russell and McPherron*, 1973; *Green*, 1984, *Clúa de Gonzalez et al.*, 1993] and is still under study. The underlying physical explanations for this behavior can be applied to specific forecasting situations, as is discussed below. However, a climatological forecast can include these inherent trends even when a specific solar wind disturbance has not been identified. Monthly Fredericksburg climatology tables are a component in SESC forecasts, and "sample climatology" (average conditions observed during the forecast time frame) is a standard for forecast comparison.

A common, simple forecast technique is persistence: the assumption that tomorrow's conditions will mimic today's. This is a respected maxim of weather forecasting that is used as a standard of comparison for SESC forecasts. As is shown below, SESC forecasts are usually more accurate than those that would be obtained using persistence alone.

TABLE 4. Number of Disturbed Days in Solar Cycle 21

Daily Geomagnetic Ap Index (Lower Limit)	*Number of Days*	*Percent of All Days*
$Ap \geq 30$	417	11%
$Ap \geq 50$	128	3%
$Ap \geq 100$	18	0.5%

Another forecasting technique is 27-day recurrence. The recurrence technique builds on the knowledge that the Sun rotates once approximately every 27 days, and assumes that stable streams of geoeffective solar wind will return like a rotating searchlight. Long-term spectral analyses of the *Ap* index [*Fraser-Smith*, 1972; *Clúa de Gonzalez*, 1993] as well as of the interplanetary field [*Gonzalez and Gonzalez*, 1987] show this 27-day peak. Recurrence is not reliable; however, it is particularly useful during the declining phase of the solar cycle, when high-speed streams of solar wind are stable [e.g., *Sargent*, 1986; *Hapgood*, 1993]. Forecast guidance based on the recurrence technique is available for daily SESC use.

There are other numerical or proxy methods for forecasting geomagnetic activity. For example, linear prediction filters have been applied to self-predicting the *Ap* index [*Thomson et al.*, 1993]. *Thomson* [1993] further applied a neural network algorithm and found some improvement in prediction accuracy. However, these techniques cannot be expected to predict storm onsets any more accurately than do the other climatological techniques.

3.2. Verification Results

K. A. Doggett (manuscript in preparation, 1995) has evaluated all of SESC's 1987–1993 forecasts. This section reports comparisons of SESC daily *A* index forecasts with the corresponding observed (hand-scaled) USGS Fredericksburg daily *A* indices. Figure 3 displays forecast-observation pairs in a format that shows the number of occurrences of matching forecasts and observations, for forecasts made a day in advance of the observation. Perfectly correlated pairs would lie on the line of slope 1; in actual fact, forecast values often exceed observed values.

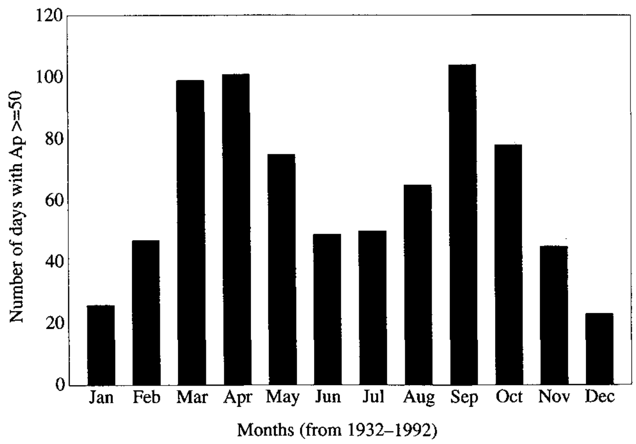

Figure 2. The *Ap* index is a global daily measure of geomagnetic activity. An index of 50 or more constitutes a major geomagnetic storm. A count of the total number of storm days between January 1932 and December 1992 in each month of the year reveals that the equinoctial months have more storms, statistically, than do solstitial months.

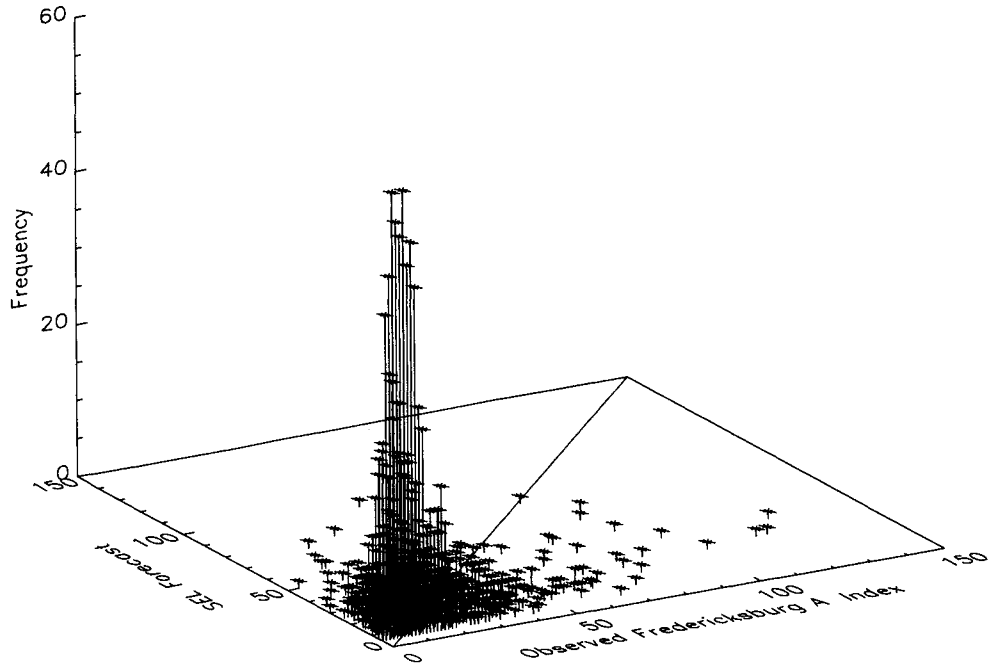

Figure 3. A good correlation between the A index forecast for Fredericksburg and the observed value would show points clustered near a line of slope 1 in the x-y plane. The linear correlation between forecasts and observation is 0.45. The data shown are the number of occurrences of daily forecast-observation pairs for 1987–1993, for forecasts made 1 day ahead.

Forecast quality can be measured in several ways. The linear correlation r is one way; over the interval 1987–1993, $r = 0.45$ (the best result would be $r = 1$). Another, "accuracy," measures the average degree of correspondence between individual forecast-observation pairs and is usually given as mean square error (MSE) or root-mean-square error (RMSE). "Bias," also called the mean error or "reliability," examines the tendency of the average forecast to be consistently greater than (over) or less than (under) that of the observed average value; zero bias is desirable.

Individual forecasters typically have a consistent bias (either to overforecast or to underforecast) that they can learn to correct once this tendency is identified. Figure 4 illustrates these measures for 1-day SESC forecasts for consecutive years since 1987. Figure 4a displays forecast accuracy, as measured by RMSE, with the actual value of the annual average of the Fredericksburg A index. The average RMSEs are all comparable to the observed values. The pattern of bias (Figure 4b) shows that the annual average SESC forecast usually exceeded the annual average observation; this was especially true during 1988, when solar activity was building up in the early years of the solar cycle. Apparently, more activity was anticipated than was observed. Geomagnetic activity was generally underforecast only during 1991, a year of extraordinary solar and geomagnetic activity. The annual correlations (Figure 4c) range between approximately 0.2 and 0.6. Correlations were lowest in 1987–1988, when solar and magnetic activity were low. The highest correlation was for 1991. An intermediate correlation was seen for 1989, the year of maximum sunspot number for solar cycle 22.

Figure 5 shows comparisons of the accuracy of the SESC forecasts with that obtained by the simple reference forecast methods of climatology, persistence, and recurrence, using annual skill scores. Skill is defined as the MSE of the reference method (e.g., climatology) minus the MSE of the SESC forecasts, all divided by the MSE of the reference. If the forecasts have equal accuracy, the skill score is zero. Positive numbers indicate that the SESC forecasts were more skillful than the reference, and negative numbers indicate that the reference was more accurate. For 1987–1993, annual average SESC forecaster accuracy a day in advance of a storm was always better than recurrence (which assumes that the observed value 27 days ago will repeat), was better than persistence (in 6 of the 7 years, and was better than sample climatology (a constant forecast of the annual average observed A index) for 5 of the 7 years. On an annual basis, the best of the simple reference forecasts was climatology, the average of all observations for that year. This result urges restraint when forecasters are tempted by circumstances to predict more extreme geomagnetic activity (quiet or storm levels) than typical, average conditions.

Does SESC forecast quality degrade as lead time increases? Every day, SESC forecasters predict the Fredericksburg A index for each of the 7 upcoming days. Figure 6 combines the data for 1989–1993 and

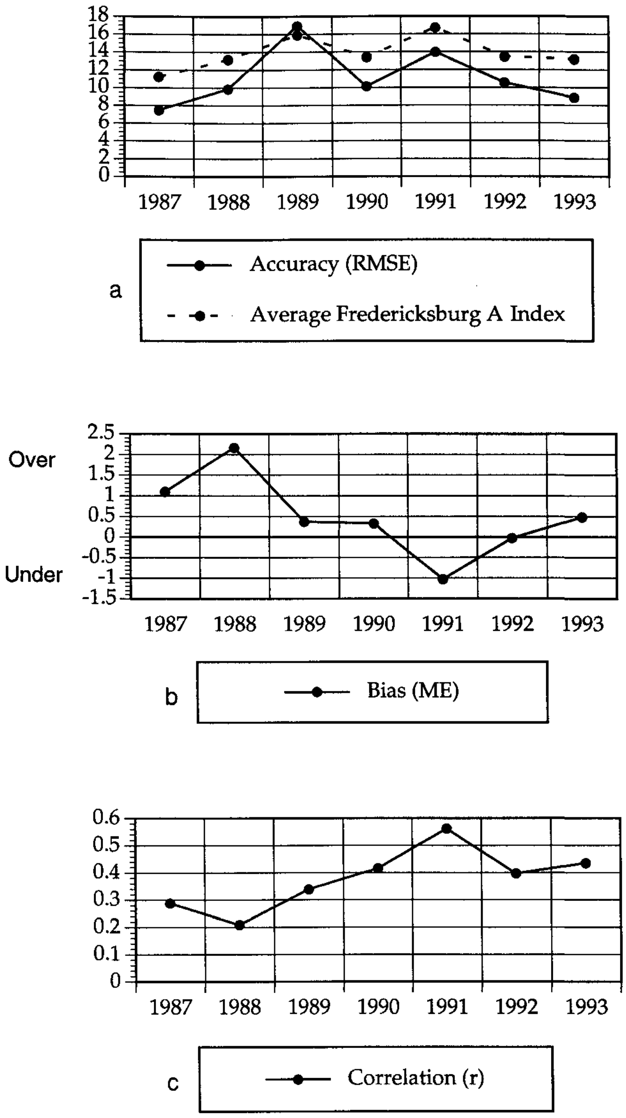

Figure 4. Annual SESC forecast verifications made one day ahead can be characterized in three ways: (a) the root-mean-square error (the actual annual average *A* index is also shown for comparison), (b) the bias toward over forecasts or underforecasts, and (c) the annual correlation coefficient.

illustrates several measures of forecast accuracy as a function of lead time. Figure 6a shows the SESC MSE and indicates that the forecast quality decreases with lead time to day 4, whereupon it effectively levels out. This pattern appears in the other panels of Figure 6 as well, especially in 6b, which shows the linear correlation coefficient for days forecast farther into the future (compare Figure 3). Figure 6c shows that SESC next-day forecasts, averaged over the past 5 years, are unbiased but become progressively more negatively biased (underforecasts) for each additional day in advance. Figure 6d shows that SESC forecasts are less accurate than sample climatology for 3 days and farther into the future.

As is shown in Table 4 and Figure 7, geomagnetic storms are relatively rare. SESC forecast accuracy is particularly disappointing when storms are considered (a storm forecast is defined as a prediction of an *A* index ≥30). Of the total number of days in 1987–1993, 173 (6.8%) were storm days. Out of 173 storm days, 47 (27%) were predicted and 126 (73%) were missed. While there were near-misses that might count as "moral victories" (e.g., a storm arrived a day earlier or later than expected, or the observed *A* index was less than 30 even though a *K* index of 6 or even higher occurred), these results indicate a lack of proficiency in the task of forecasting geomagnetic storms.

Figure 8 summarizes categories of SESC forecasts a day in advance vis-à-vis observed conditions during the 6 years 1987–1993. Forecasts of quiet conditions were generally rewarded with the occurrence of quiet conditions, and forecasts of unsettled conditions were usually followed by unsettled conditions; forecasts of active or storm conditions were less definitive.

4. SOLAR ORIGINS OF GEOMAGNETIC ACTIVITY

Prior to the availability of space-based solar optical and interplanetary solar wind data, solar flares and "M regions" served as solar progenitors of geomagnetic activity. When no flare was observed, nonrecurrent geomagnetic activity was often attributed to unseen flares on the back side of the Sun [e.g., *Dodson et al.*, 1979]. Then solar images in X ray wavelengths revealed "coronal holes," which were soon associated with high-speed solar wind streams and episodes of recurrent geomagnetic activity [e.g., *Hundhausen*, 1977]. Sector boundaries were also found to have a statistical signature in geomagnetic indices; this topic is discussed in more detail below.

Skylab's discovery of coronal mass ejections (CMEs) and their intimate association with erupting prominences gave rise to suggestions that disappearing solar filaments could predict geomagnetic activity [*Joselyn and McIntosh*, 1981; *McNamara and Wright*, 1982; *Wright and McNamara*, 1983]. However, efforts to forecast geomagnetic storms on the basis of specific flares, filament disappearances, or coronal holes usually yielded ambiguous results, and some storms had no obvious solar precursor [*Tang et al.*, 1985; *Joselyn*, 1986a; *Neugebauer*, 1988]. To further complicate matters, flares, coronal holes, and filament disappearances far outnumber geomagnetic effects. It has also been suggested that separate forms of solar activity are not necessarily independent. For example, *Dodson and Hedeman* [1972] noted an apparent relationship between flares and filament disappearances, and *Sheeley et al.* [1983] noted that filament disappearances sometimes accompany the birth of coronal holes. This incoherent picture of the solar origins of geomagnetic activity underlies the poor record of geomagnetic forecast verification.

Lately, however, the picture has been improving.

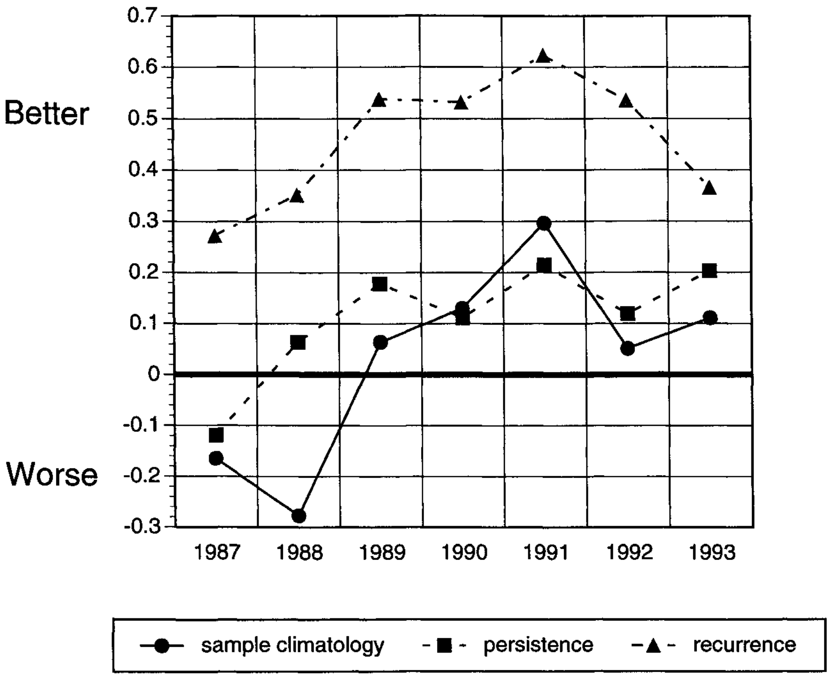

Figure 5. SESC forecasts made one day in advance are compared with simple reference forecasts. If both forecasts are similarly accurate, the score is zero; if the SESC forecast is more accurate, the score is positive. Since 1989, SESC forecasts have beaten" the simple forecasts of climatology, persistence, and recurrence.

For example, the value of solar flares as a predictor of nonrecurrent geomagnetic activity has been formally challenged, and a new paradigm is emerging that places coronal mass ejections in the central role [*Gosling et al.*, 1990; *Kahler*, 1992; *Gosling*, 1993]. The forecasting task remains difficult, however: first the CME must be identified; then it must be proven to drive or become an interplanetary disturbance [*Wilson and Hildner*, 1984; *Webb*, 1993].

Coronal mass ejections at 1 AU generally have distinct plasma and field signatures by which they can be distinguished from ordinary solar wind [*Gosling*, 1990]. The phrase "magnetic cloud" [*Klein and Burlaga*, 1982; *Burlaga*, 1991] presents a descriptive image of a CME-caused interplanetary disturbance. The cloud carries an intrinsic magnetic field, often with the characteristics of a flux rope [*Marubashi*, 1986]; it interacts with other solar wind structures and with the ambient medium [*Burlaga et al.*, 1987; *McComas et al.*, 1989]. Magnetic clouds have been identified with geomagnetic effects at Earth [e.g., *R. M. Wilson*, 1987; 1990; *Zhang and Burlaga*, 1988; *Gosling et al.*, 1991]. Other measureable characteristics of potentially geoeffective parcels of solar wind include bidirectional electron heat flux events, interpreted as populations of electrons traveling along interplanetary magnetic field lines which either are rooted at both ends in the Sun or else are on closed loops entirely disconnected from the Sun [*Gosling et al.* 1987], and, similarly, bidirectional proton events [*Marsden et al.*, 1987]. Some noncompressive density enhancements (high densities observed when the solar wind bulk flow speed is nearly constant or falling) [*Gosling et al.*, 1977], which have been associated with coronal streamers, may also have a transient origin.

Of all of the characteristics measured in the solar wind, it is now well understood that a necessary and sufficient condition for geomagnetic storms is a strong southward component of the interplanetary magnetic field, B_z [e.g., *Russell et al.*, 1974; *Gonzalez and Tsurutani*, 1987; *Gonzalez et al.*, 1994, and references therein]. This southward component "reconnects" or couples with the northward pointing intrinsic geomagnetic field, in intuitive agreement with the principle that opposite magnetic fields attract, while like fields repel. Under "attractive" conditions, solar wind energy is converted into magnetic energy stored in a distorted geomagnetic field. It is the release of this energy, in a variety of forms, that becomes manifest in geomagnetic activity. Other relevant solar wind parameters besides the interplanetary field are high speed and, perhaps, increased momentum flux. Can this new paradigm of CMEs as the source of geoeffective solar wind be employed to improve geomagnetic forecast accuracy for transient events? The next section examines this question; it is followed by a review of our present understanding of the solar source of recurrent geomagnetic activity.

4.1. CMEs and Nonrecurrent Geomagnetic Activity

The release of mass and energy into the solar wind accompanying CMEs provides the raw material for nonrecurrent geomagnetic activity. Thus if a CME is observed or suspected, there is reason to consider the likelihood of a geomagnetic storm. Coronagraphs at Earth observe CMEs beyond the rim of the Sun, pro-

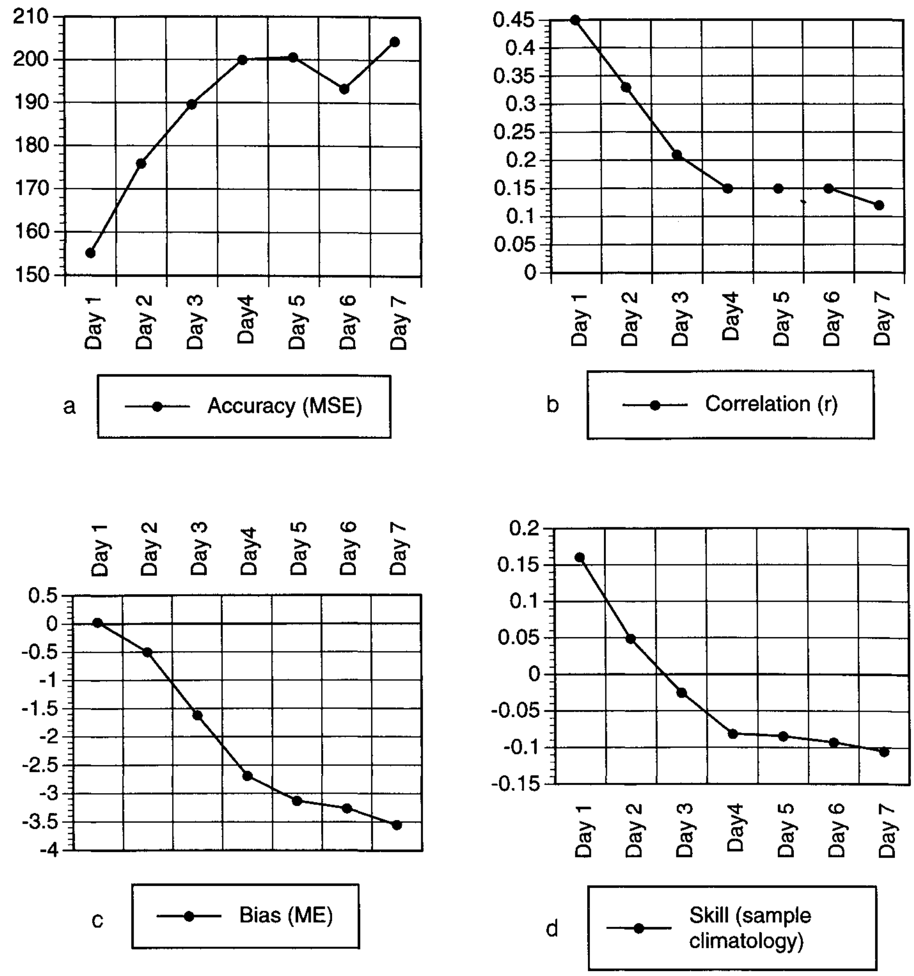

Figure 6. Various characterizations of SESC forecasts made more than 1 day ahead are shown. These are (a) accuracy or mean square error, (b) the correlation coefficient, (c) bias (negative values indicate an underforecast), and (d) skill against climatology (the simple average of observed A indices). Data shown are for 1987–1993.

jected into the plane of the sky. CMEs seen in this way may not be geoeffective because they are apparently aimed away from Earth. However, if the CME is large (the average width of approximately 1200 CMEs observed by the Solar Maximum Mission (SMM) was 47° [*Hundhausen*, 1993] or its release site is sufficiently close to solar central meridian, an associated interplanetary magnetic cloud could impact Earth and spawn geomagnetic effects.

The first problem is that of recognizing the existence of a CME at all. Several proxy signatures of CMEs have been identified. These are long-duration solar X ray events (LDEs), filament disappearances, certain radio sweeps usually accompanying major flares, and solar energetic particles. However, since only 66% of the CMEs observed by SMM during 1980 could be associated with reported solar activity [*Webb and Hundhausen*, 1987], the absence of a CME proxy does not imply the absence of a CME.

In an effort to evaluate the reliability of X ray events as a CME proxy, *Sheeley et al.* [1983] examined the enhanced soft X ray emission accompanying flares and filament eruptions; they found that longer-duration X ray events were more likely to be associated with CMEs; events lasting 6 hours or more were always associated with CMEs, but some shorter bursts also had CMEs. Unfortunately, the converse is not true: many CMEs have no X ray signature [e.g., *Webb and Hundhausen*, 1987]. In SESC practice, an X ray event, often a flare, is flagged as a possible CME when the time between X ray maximum and recovery to half of the peak amplitude is 30 min or more. Because the importance of a flare in hydrogen light was found to be a poor indicator of its interplanetary effects [*Schwenn*, 1983], the duration of the X ray signature is helpful to alert forecasters of a possible geoeffective event.

Metric radio bursts, a common component of significant solar flares, are variously associated with CMEs. The relationship between type II bursts and CMEs is not definitive [*Kahler*, 1992]. For example, *Sheeley et al.* [1984] found that 70% of the type II bursts on their list were associated with CMEs but that

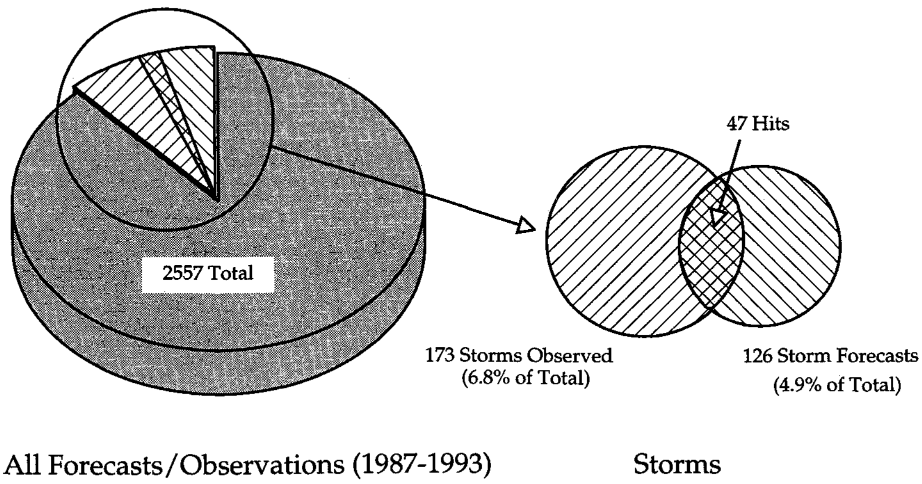

Figure 7. The observed A index for most days between 1987 and 1993 was less than 30, the threshold for a storm. Of the 6.8% of the days that were storm days, only 27% (47 of 173) were forecast. Of the 126 storms that were forecast, 63% were false alarms.

some CMEs, even fast ones (super Alfvénic, with velocity v of >400 km s^{-1}), were not. These bursts are neither necessary nor sufficient for the occurrence of interplanetary shocks [*Sheeley et al.*, 1985], nor are they well correlated with geomagnetic sudden impulses or geomagnetic storms. When type IV broadband radio emission occurs, it is generally associated with CMEs, especially with fast ones [*Cane and Reames*, 1988]. Type III radio bursts may presage CMEs. *Jackson et al.* [1980] looked at type III burst rates preceding known CMEs and found a peak about 8 hours prior to CME initiation. However, the inverse study has not been successful: type III radio bursts, per se, are not a helpful diagnostic for geomagnetic activity. SESC forecasters use type II and type IV radio bursts as possible CME proxies but do not use type III bursts.

Prominence eruptions and filament disappearances are strongly associated with CMEs [*Sheeley et al.*, 1975; *Munro et al.*, 1979; *Wilson and Hildner*, 1986; *Webb and Hundhausen*, 1987]. *Wright and Webb* [1990] searched for signatures in solar wind data at 1 AU 2.5–5.5 days following large filament disappearances and concluded that several CME-associated,

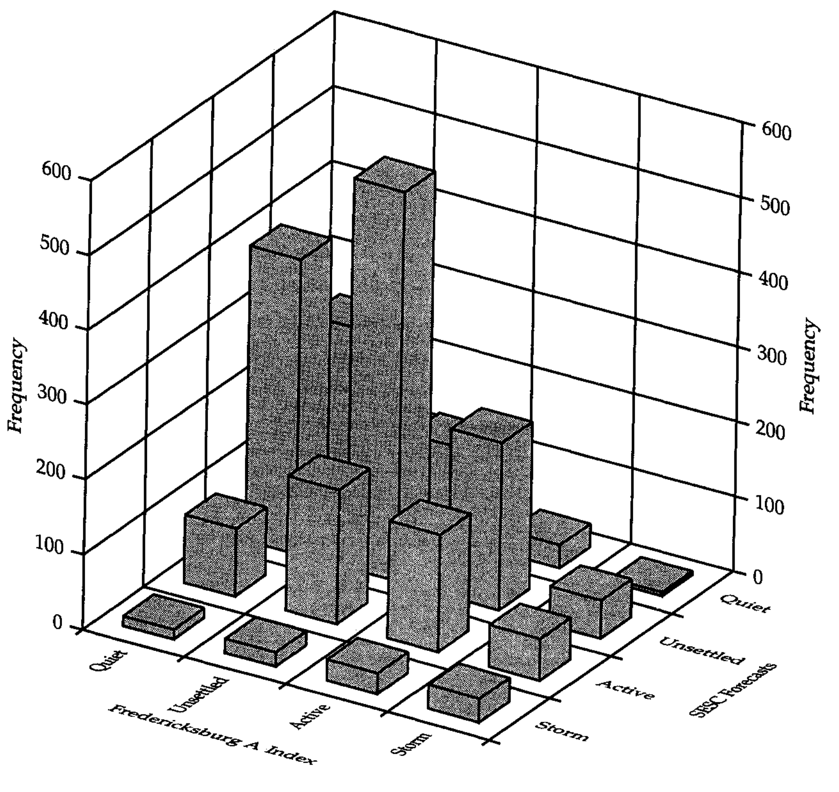

Figure 8. A pictorial representation shows SESC success in forecasting categories of geomagnetic activity, defined in Table 3. Data shown are for 1-day forecasts, 1987–1993.

interplanetary disturbance features (shocks, increases in solar wind proton density, and increases in magnetic flux density) were evident, lending credence to their value as CME proxies.

Prompt solar energetic particle (SEP) events, interplanetary particle streams of MeV energies, are favorably associated with CMEs [*Kahler et al.* 1978, 1984]. Long-duration particle events (lasting for days) are even more strongly associated with CMEs [*Kahler*, 1993b]; these energetic protons are almost certainly produced in interplanetary space by CME-associated shock structures, with or without a flare [*Reames*, 1993].

A good association between energetic proton events and subsequent geomagnetic storms can be shown [e.g., *Cliver and Crooker*, 1993]. Between 1976 and 1989, 62% of the 92 SESC solar proton events (strictly defined as an episode of at least 30 min duration with a flux of more than 10 protons cm^{-2} s^{-1} of energies exceeding 10 MeV) preceded geomagnetic storms ($Ap \geq 30$) within 2–3 days; 75% of the larger events (peak fluxes exceeding 100 flux units) were followed by storms. Thus of all the CME proxies, the observation of a proton event at Earth offers the best warning of a possible geomagnetic storm within 24–72 hours.

"Remote sensing" methods that identify coronal transients and interplanetary disturbances have been reviewed by *Bird and Edenhofer* [1990]. Within 0.5 AU, Doppler scintillation measurements of spacecraft telemetry signals exhibit transients that have been matched with interplanetary shocks [*Woo et al.*, 1985], in situ observations of magnetic clouds [*Woo and Schwenn*, 1991], CMEs [*Woo*, 1993], and compressed plasma at the leading edges of high-speed streams [*Woo and Gazis*, 1993]. Doppler scintillation can provide data potentially useful for forecasting purposes, but this method requires an advantageously located interplanetary probe (it is a point measurement) and further interpretation because, as in the case of coronagraph CMEs, the information is integrated along the line of sight.

Beyond 0.5 AU, ground-based interplanetary scintillation (IPS) observations of radio sources that are spread over an extended portion of the celestial sphere have been used to infer transient interplanetary disturbances from daily maps of the spatial distribution of high- and low-density fluctuation regions [e.g., *Erskine et al.*, 1978; *Watanabe and Schwenn*, 1989, and references therein]. Physical interpretations of the IPS fluctuations are disputed [e.g., *Bravo et al.*, 1991; *Moore and Harrison*, 1994], and attempts to use IPS observations in an operational mode have not met with success [*Leinbach et al.*, 1994].

Finally, there is an optical method to track interplanetary disturbances. Zodiacal light photometers on the Helios spacecraft imaged coronal mass ejections and traced them out to 0.5 AU [*Jackson and Leinert*, 1985]. A second-generation scattered-light optical imager has been proposed that could operate from a near-Earth polar-orbiting platform [*Jackson et al.*, 1991]. A weakness of all of the remote-sensing methods is that they do not include information about the direction of the interplanetary magnetic field, the most important parameter for geoeffectiveness.

Once a CME is suspected, especially one with a photospheric signature, an assessment of its probable internal magnetic structure is the critical next step. This question involves the prediction of a strong southward, out-of-the ecliptic magnetic field component. *Burlaga et al.* [1987] investigated 17 large geomagnetic storms with adequate solar wind data that occurred between 1972 and 1983. They determined that there is no single cause of large geomagnetic storms. Some storms were linked with magnetic clouds, some were caused by interacting (compound) streams, and some could be identified with both. The largest storm, on July 13, 1982, was caused by a compound stream. *Tsurutani et al.* [1988] investigated the origins of the southward fields that were the ultimate cause of 10 intense geomagnetic storms in 1978–1979. The various causes included southward fields entrained in a cloud, shock compression of preexisting southward fields, turbulence behind shocks, and draping over a noncompressive density enhancement. *Tang et al.* [1989] looked for the corresponding solar sources and found plausible CMEs or CME proxies for each: either long-duration X ray flare events or prominence eruptions. However, these authors conclude that the solar sources of intense geomagnetic activity do not have to be optically large or energetic solar events.

Efforts to use observed solar magnetic field patterns to predict B_z at Earth have had inconsistent success. *Pudovkin and Chertkov* [1976] found an association of large-scale southward fields (and not northward fields) at flare sites with subsequent geomagnetic storms. *Tang et al.* [1985, 1989] found no simple relationship between the magnetic orientation at flare sites and the solar wind B_z orientation at Earth.

The possibility of using magnetic field orientation near disappearing filaments to infer the interplanetary magnetic field direction is conceptually more favorable than using flares because filaments are generally large, quasi-linear features that lie on large-scale magnetic inversion lines [*McIntosh*, 1972]. Close associations have been made between filament disappearances, CMEs, and "flux rope" magnetic structures (smooth rotations of the magnetic field vector over a large angle) in clouds [*Wilson and Hildner*, 1986; *Marubashi*, 1986; *Wilson*, 1990]. *Wright* [1986] defined a coordinate system based on the size, location, and photospheric orientation of the erupting filament and found some tendencies for geoeffective filaments to have a preferred orientation; however, the results were not definitive.

TABLE 5. Association of DSF Orientation With Subsequent Geomagnetic Storms

	Orientation							
	+ — −	− — +	+ \ −	− \ +	+ / −	− / +	− | +	+ | −
Number of cases	6	7	5	7	4	4	6	7
Number of storms	2	0	2	2	1	2	0	2

DSF, filament disappearance.

Bothmer and Schwenn [1994] studied the relationship between the magnetic field orientation of disappearing solar filaments and magnetic clouds observed by Helios; they concluded that eruptive prominences were a probable source of the magnetic clouds and that the magnetic flux rope structure of the clouds was the same as that of the associated filament. This suggests that an analysis of the orientation of the disappearing solar filament would be useful as predictive guidance. However, an investigation of the magnetic orientation of 46 major filament disappearances (DSFs), filaments of 20° or more in extent that are "normal" or "dark" in hydrogen spectroheliograms, near solar central meridian in 1979 produced the discouraging results shown in Table 5. In this table the orientation of the filament is shown as a bar, horizontal, vertical, or slanted to show the approximate appearance of the filament on the disk, along with the appropriate polarity, positive (+) or negative (−), of the solar magnetic field on either side of the filament. Presumably, the most favorable orientation of a filament would be east-west (horizontal) with positive polarity north of the filament; if the arcade of magnetic field lines arching above the filament preserved its structure as it propagated or extended to Earth, the interplanetary magnetic field would be predominately southward, and geomagnetic activity would occur. In the table the DSF was associated with a storm ($Ap \geq 30$) if a storm occurred within 3–5 days of the date that filament was last seen (this assumes an average travel speed of approximately 600–350 km s^{-1}). No attempt was made to exempt storms that might have been due to other causes, so the number of storms counted may be overestimated. The results of this limited but practical test using good examples of filament disappearances were that no storms were associated with the least favorable orientation (negative fields north of an east-west filament), but that few storms could be associated with the most favorable orientation. Another clear result is that filament disappearances, of any orientation, are not a reliable predictor of geomagnetic storms.

Thus in the absence of additional information, the observed filament orientation per se does not provide definitive predictive guidance. Perhaps, however, using solar photospheric fields is not an appropriate approach to improving forecasting. *Kahler* [1992] pointed out that the filament field generally lies at a large angle to the overlying field that may be the dominant orientation in the CME plasma. He questioned whether we know the topology of the appropriate coronal fields and, if we do, whether large-scale eruptive coronal fields maintain either their integrity or direction in the interplanetary medium.

Hoeksema and Zhao [1992] extrapolated the photospheric magnetic field to the high coronal altitudes that may be regarded as the base of the solar wind and, for three of five cases, matched northward or southward orientations for the active-region CMEs in their study with the same orientation at Earth. However, *Kahler* [1993a] criticized several of their assumptions (including the relationship of the flares to the CMEs); he further investigated the geomagnetic consequences of the simplest possible coronal field–interplanetary orientation: the solar dipole field at solar minimum. He reasoned that if the dipole orientation were preserved even approximately in the coronal ejecta, then the time (18 months) of those solar minima for which the solar dipole field points southward (the northern solar pole currently has a positive polarity) would, statistically, be more geomagnetically active than that of minima with the reversed orientation. Five minima of each orientation were analyzed; each set had approximately the same number of storms. No evidence of solar cycle dependence of B_z was found, implying that it is not reasonable to expect that B_z can be inferred from the more complicated coronal fields near solar maxima [*Kahler*, 1993a].

Some conditions of interplanetary propagation that lead to geoeffective solar wind are not apparent in solar observations. While interplanetary clouds occur in both fast and slow transient flow [*Burlaga et al.*, 1987; *Gosling et al.*, 1987], most of the largest geomagnetic storms are associated with storm sudden commencements, which are primarily caused by interplanetary shocks. Most interplanetary shocks can be associated with fast (>500 km s^{-1}) CMEs [*Sheeley et al.*, 1985; *Schwenn*, 1986], and, importantly for geomagnetic effects, the most intense interplanetary fields follow shocks [*Burlaga and King*, 1979]. Shock drivers, the interplanetary material responsible for the formation of the shock, generally extend up to 100° in longitude and are centered on the presumed solar source longitude; 80% of shocks from presumed sources near the central meridian are followed by drivers [*Richardson and Cane*, 1993; *Richardson et al.*, 1994]. *Kahler* [1992] reviewed the characteristics of high-speed driver-gas plasmas behind interplanetary shocks. *Cane et al.* [1986] identified six interplanetary shocks associated with filament eruptions, showing that rapid release of energy is not necessary for the formation of an interplanetary shock. *Gosling et al.* [1991] found that about three fourths of 37 geomagnetic storm events between August 1978 and October 1982 were associated with Earth passages of CMEs and their related shocks; however, only half of the observed CME shocks resulted in a storm. Of interest for prediction, draping of the ambient interplanetary field about the rapidly ejected material could lead to an increased out-of-the-ecliptic (northward or southward) magnetic field [*Gosling and McComas*, 1987], but there is no a priori way to predict whether draping effects will be substantial in any given situation [*McComas et al.*, 1989].

4.2. Recurrent Geomagnetic Activity

Ever since geomagnetic activity was routinely charted, it has been known that some activity recurs approximately every 27 days [e.g., *Bartels*, 1963]. Subsequent studies found that 27-day recurrence is most significant in the declining phase of even-numbered solar cycles [e.g., *Sargent*, 1986; *Hapgood*, 1993]. These recurrent geomagnetic disturbances were associated by *Neupert and Pizzo* [1974] with solar coronal holes observed by OGO 7.

Skylab's X ray images of the Sun, together with interplanetary plasma data from other spacecraft, allowed rapid progress in relating coronal holes with high-speed, low-density solar wind [*Nolte et al.*, 1976]. Understanding of the relationships between coronal holes, high-speed solar wind streams, and geomagnetic disturbances was further developed by *Sheeley and Harvey* [1981] and *Legrand and Simon* [1991]. *Sheeley and Harvey* [1981] noted that the speed of streams from coronal holes is solar cycle dependent (greatest in the years of cycle decline, when the holes are largest and extend across the solar equator). They also substantiated the presence of the Russell-McPherron effect in coronal hole polarity [*Russell and McPherron*, 1973], namely, that negative polarity holes (with the magnetic field pointing inward toward the solar surface) are more geoeffective in the spring and positive holes are more geoeffective in the fall because the tilt of the geomagnetic axis with respect to the rotational axis transforms an interplanetary field lying in the ecliptic into a field with an apparent southward field component in the magnetospheric coordinate frame. Seasonal variations in geomagnetic activity are discussed below.

Wang and Sheeley [1988, 1990] quantitatively modeled solar wind expansion from coronal holes, thereby predicting daily solar wind magnetic polarity and speed at Earth. Given this relatively advanced theoretical foundation, how useful are coronal holes for predicting geomagnetic activity?

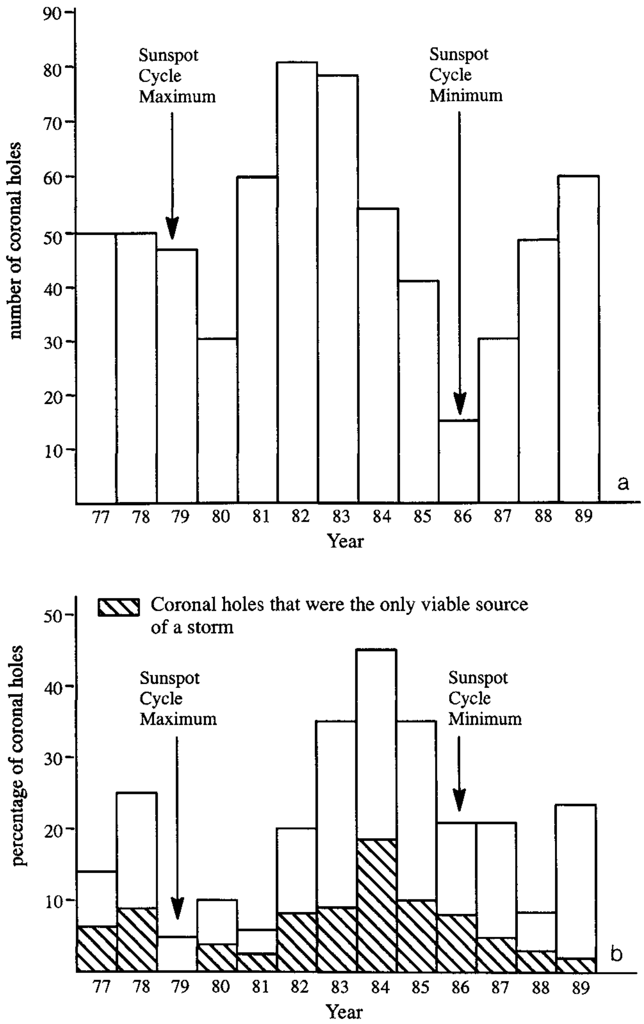

Figure 9. (a) The annual number of coronal holes observed using He 1038-nm images illustrates the characteristic pattern of minima of occurrence during sunspot cycle minimum and maximum, and a peak during the years of sunspot cycle decline. (b) The annual percent of the observed low-latitude coronal holes that could be associated with geomagnetic storms is plotted against the portion that were solely associated with storms (no other viable source was observed).

Figure 9 shows the correspondence between coronal holes and geomagnetic storms ($Ap \geq 30$). Because geoeffective coronal holes are located at low geomagnetic latitudes [e.g., *Watari*, 1990], the coronal holes counted in Figure 9a were those in each solar rotation that extended to within 30° of the helioequator; many cross the equator. These holes were identified from the synoptic charts published monthly in *Solar Geophysical Data* (based on He 1083-nm images provided by the National Solar Observatory in Kitt Peak, Arizona) and were not cross-checked with published coronal hole catalogues such as that by *Sanchez-Ibarra and Barraza-Paredes* [1992]. In Figure 9b, holes were as-

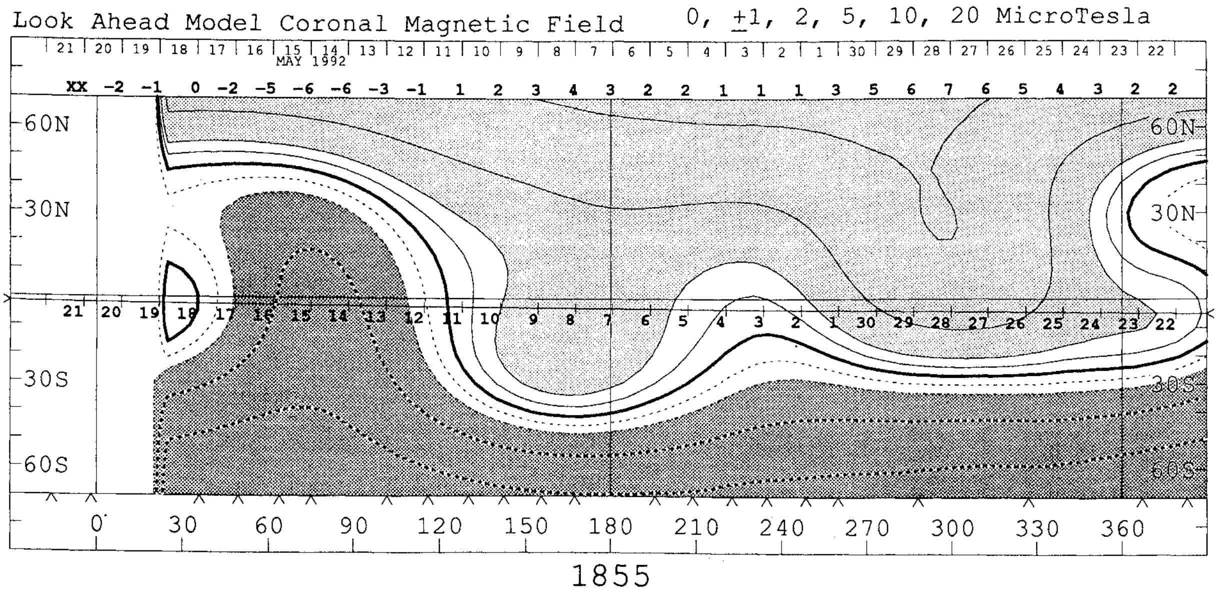

Figure 10. The computed coronal field at the source surface predicts the configuration of the heliospheric magnetic field. The heavy line shows the location of the neutral sheet, where the polarity of the radial magnetic field reverses. Solid contours and light shading indicate positive field (away from the Sun), while dashed contours and dark shading show negative regions. The radial projected path of Earth lies just above the helioequator; dates denote the time of central meridian passage of that longitude. The field strength at the subterrestrial point appears in the upper margin. The data shown are for April 22 to May 21, 1992, Carrington rotation 1855 (figure taken from *Hoeksema* [1993]).

sociated with storms if the storm began within 48–72 hours following the central meridian passage of the center of the hole (this assumes that the relevant high-speed stream speed was between approximately 600 and 800 km s^{-1}). Some storms had no other obvious source (such as a filament disappearance or flare-associated solar activity) besides the sole presence of the coronal hole. Whenever possible, solar wind data were used to confirm "sole-source" coronal holes by checking for the presence of a high-speed stream with radial interplanetary field polarity matching that of the hole. On average, only 20% of the observed coronal holes were associated with storm-level activity. However, the range of association for the years examined was from 4% to 44%; the peak occurred during the waning years of solar cycle 22, as expected. The percentage of solely associated coronal holes is smaller and is diminished by the requirement that there be no other obvious source for the storm.

The conclusion offered by Figure 9 is that coronal holes are useful as a diagnostic factor in geomagnetic forecasting but like filament disappearances, are not especially reliable. More information (e.g., the interplanetary magnetic field) and understanding are needed. In particular, we need to know if the terrestrial effects are primarily a result of the high-speed solar winds associated with coronal holes or if they are a consequence of the interactions between differing solar wind flows as was suggested by *Crooker and Cliver* [1994]. These complexities are addressed in the next section.

4.3. The Ambient Solar Wind and Geomagnetic Activity

The ambient (i.e., quasi-steady state) solar wind is assumed to expand freely from a nonuniform "source surface" at a few solar radii in the outer solar corona, carrying entrained coronal fields with it. Even if transient flows are not considered, there is structure in the quiet solar wind at the source surface, as a result of solar wind acceleration mechanisms (e.g., high-speed streams from coronal holes), and beyond, owing to interactions between flows of differing speed and differing magnetic orientation [*Neugebauer*, 1983].

Figure 10 illustrates the results of a calculation described by *Hoeksema et al.* [1982] to estimate the strength and polarity of the interplanetary magnetic field in the high solar corona at the base of the solar wind. The calculation uses a potential field model with daily magnetic maps of the photosphere; it is available routinely and promptly from the Wilcox Solar Observatory in California. An obvious feature in this figure is the trace of the heliospheric current sheet, a low-speed, enhanced-density feature marking the transition between regimes in the solar wind where the underlying coronal field points predominantly either toward or away from the Sun. *Wilcox and Ness* [1965] observed this apparent discontinuity in in situ solar wind data and identified it as a solar sector boundary (SSB). SSBs are described by *Behannon et al.* [1981, p. 3273] as "the ecliptic plane intersections of a warped global current sheet that surrounds the Sun near its equatorial plane." Crossings of the helio-

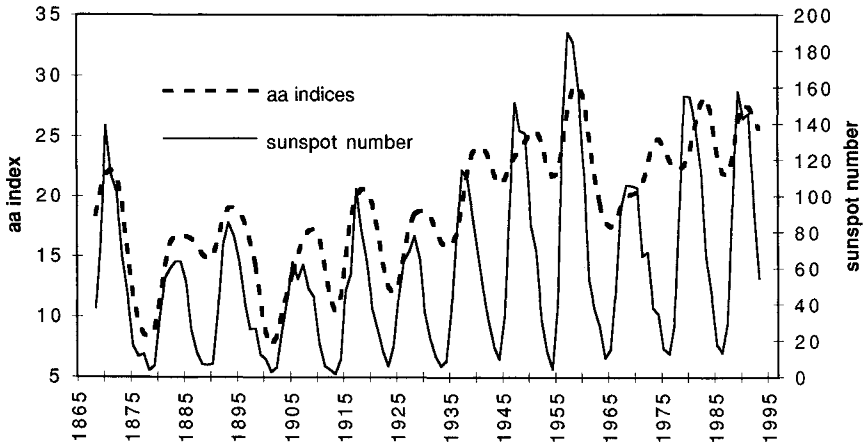

Figure 11. The annual average *aa* index for 1868 through 1993, smoothed and overlain onto the annual average sunspot number.

spheric current sheet offer an easily recognized fiducial for superposed epoch studies to look for associations with geomagnetic activity [e.g., *Hirshberg and Colburn*, 1973; *Lundstedt et al.*, 1981; *Arora and Rangarajan*, 1981; *Perez-Enriquez and Mendoza*, 1993]. On average, a slight enhancement in activity is found following the passage of an SSB. However, many SSB crossings can be associated with quiet conditions [*Joselyn*, 1990]; this is consistent with the slow flow and low values of the interplanetary magnetic field at the current sheet.

The more general case of ambient solar wind structure is a corotating interaction region (CIR), arising from any gradient in solar wind speed at the source. If the gradient is large, regions of compression and rarefaction develop as the solar wind flows away from the Sun. As reviewed by *Schwenn* [1990], these stream fronts and interfaces compress and deflect the interplanetary magnetic field. In some cases the CIR steepens into a shock, visible in geomagnetic records as a sudden impulse as the structure sweeps past Earth.

Some geomagnetic activity cannot be associated with high-speed streams, boundary interfaces, or transient flows. That portion of the solar cycle without coronal holes or solar activity occurs just after sunspot minimum and corresponds with the minimum average levels of the 11-year geomagnetic cycle as shown in Figure 11. The solar wind at those times is characterized by low speeds and temperatures and has been associated with quiescent, near-equatorial coronal streamers [*Feldman et al.* 1981]. Solar wind flow may be influenced by multiple, interacting current sheets from multiple helmet streamers at the base of the corona [*Crooker et al.* 1993], or, coronal mass ejections propagating through the streamer belt [*Crooker and Cliver* 1994]. Geomagnetic activity could then follow from a favorable combination of ambient conditions and magnetospheric receptivity.

5. MAGNETOSPHERIC INFLUENCES

The importance of magnetospheric control of geomagnetic disturbances is evidenced by seasonal patterns in geomagnetic activity and storm occurrence. Figure 2 illustrated the striking tendency for storms to occur in the equinoctial months. This pattern was noted in early studies of geomagnetic activity [e.g., *Bartels*, 1963]. Although discussions continue, it is well established that storms are seasonally modulated primarily as a consequence of the angle between the dipole geomagnetic field axis and Earth's rotational axis [*Russell and McPherron*, 1973]. SESC forecasters use this effect to predict coronal hole geoeffectiveness. In actual practice, shown in Table 6, coronal holes of either polarity can be associated with storms throughout the year even though there is a tendency for negative polarity holes to be more geoeffective in northern hemisphere spring, February–April, and positive polarity holes to be more geoeffective during August–October.

Crooker et al. [1992] and *Cliver and Cooker* [1993] validated the seasonal tendencies of transient (CME) events. *Phillips et al.* [1993] also investigated seasonal effects for CME-associated storms but found season to be a predictor secondary to solar wind speed and magnetic field. They also found evidence that pre-existing geomagnetic conditions influence storm am-

TABLE 6. Storms Attributed Solely to Coronal Holes, 1976–1989

Polarity of Coronal Hole	*February–April*	*May–July*	*August–October*	*November–January*	*Total*
Positive	7	0	12	4	23
Negative	8	4	4	2	18

plitude: except for the strongest storms, more disturbed preexisting conditions correlate with stronger storms. Is this a magnetospheric effect? Quantitative guidance is lacking.

6. DISCUSSION

The effects of geomagnetic activity on technological systems are becoming more important as components are miniaturized and as operating margins thin. There is also an increasing dependence on systems resident in space, where the levels of fluctuation in the ambient environment, primarily in association with geomagnetic activity, may change by orders of magnitude (e.g., energetic electron fluxes at geosynchronous orbit). Increased demands for appropriate descriptions and accurate predictions of geomagnetic disturbances are emerging. This need can be addressed in several ways:

Present data and knowledge can be reformulated in more applicable forms. For example, the SESC has begun expressing forecasts in terms of the probability of expected outcomes [*Balch*, 1990]. In addition to the value of the expected Fredericksburg *A* index for tomorrow, the likelihood of occurrence of active conditions, a minor storm, or a large (i.e., major or severe) storm is also given. This formulation has the advantage of informing the user that a storm may occur, even when the prudent forecast calls only for unsettled or active conditions. It also provides operators who use cost-loss decision methods more quantitative information with which to work.

Another way to be more effective in using our current data and knowledge is by developing "specification" or nowcasting models that enable synthesis and vizualization of the space environment as a system. An example is the MSFM, developed for use as a operational tool [*Bales et al.*, 1993; *Freeman et al.*, 1993].

Another response to improving geomagnetic forecasts is to discard present methodologies and search for new ones. This response is appropriate to the research community but is more difficult for operational service organizations, which are reluctant to adopt concepts and algorithms that have not been thoroughly tested. In addition, new concepts are often based on new data that have been gathered in research campaigns and are not routinely available. It usually is very expensive to acquire new sensors on new observation platforms. One operationally focused way to seek new forecasting paradigms is to employ new analysis techniques on existing data streams. An example is the application of artificial intelligence methodologies to solar-terrestrial data [e.g., *McPherron*, 1993].

Finally, new observations are being sought. One data set that proved in the past to be valuable for nowcasts was the plasma and magnetic field data from ISEE 3, which was available for operations in real time in 1979–1980 [*Joselyn et al.*, 1981]. This suite of data has again become available, for a few hours each day, with the successful launch of the NASA WIND spacecraft in late 1994. The WIND data are most helpful for short-term (i.e., 1 hour) alerts of severe geomagnetic storms but also enable forecasters to identify and chart quasi-steady structures such as high-speed streams and the heliospheric current sheet. An Earth-directed CME monitor [e.g., *Hoeksema*, 1992] is now being discussed. This technique would place one (or two) coronagraphs approximately 90° away from Earth, in the plane of the ecliptic. In this way, CMEs directed toward Earth could be seen and their velocities could be estimated.

7. SUMMARY

Are accurate geomagnetic forecasts, a day or several days in advance of storm onset, possible with the present knowledge and data? Unfortunately, present capabilities are limited and are often bested by simple forecasting schemes such as climatology. However, we are making rapid progress, having learned several important things. By analyzing forecast verifications, we have been able to discard a paradigm, solar flares as the source of nonrecurrent geophysical disturbances, that does not verify adequately. In its place, a new concept is building. We are looking above the solar surface into the corona for storage and release of mass and energy and then considering how these new releases of mass and energy act upon and merge into the solar wind flow to produce geoeffective topologies.

Further, we now appreciate that Earth and its magnetic field use several physical mechanisms to extract energy. The magnetosphere responds to details of the solar wind (specific magnetic field orientations weighted by atypical plasma parameters, such as extraordinary velocity or density [e.g., *Rostoker et al.*, 1987]. While new observations (X ray imaging, interplanetary remote sensing, in situ measurements) are contributing fresh insights into the dynamics of the system, it is difficult indeed to predict solar wind parameters in precise enough detail at the position of Earth to be able to forecast geomagnetic activity a day or more in advance. Nearby, real-time observations of the solar wind offer the best opportunity for improved geomagnetic warnings, but only a few minutes to hours in advance.

ACKNOWLEDGMENTS. K. A. Doggett (NOAA Space Environment Laboratory) provided much of the data and analysis of SESC forecast verifications. S.-I. Watari (Hiraiso Solar Terrestrial Research Center) contributed to the analysis of the geoeffectivity of solar proton events.

The editor responsible for handling this paper is Thomas Cravens. He thanks two technical referees, Gordon Rostoker and Marcia Neugebauer, and the cross-disciplinary referee, Duncan C. Agnew.

REFERENCES

Allen, J., H. Sauer, L. Frank, and P. Reiff, Effects of the March 1989 solar activity, *Eos Trans. AGU*, *70*, 1479, 1989.

Arora, B. R., and G. K. Rangarajan, Temporal variation in the geomagnetic response to IMF sector boundary passage, *J. Geophys. Res.*, *86*, 3369, 1981.

Axford, W. I., The interaction between the solar wind and the magnetosphere, in *Physics of Geomagnetic Phenomena*, vol. 1, edited by S. Matsushita and W. H. Campbell, p. 1243, Academic, San Diego, Calif., 1967.

Balch, C., A probability forecast for geomagnetic activity, in *Proceedings of the 1989 Solar-Terrestrial Predictions Workshop*, vol. 2, p. 13, Natl. Oceanic and Atmos. Admin., Boulder Colo., 1990.

Bales, B., et al., Status of the development of the Magnetospheric Specification and Forecast Model, in *Proceedings of the 1992 Solar-Terrestrial Predictions Workshop*, vol. 2, p. 467, Natl. Oceanic and Atmos. Admin., Boulder, Colo., 1993.

Bartels, J., Discussion of time variations of geomagnetic activity indices *Kp* and *Ap*, 1932–1961, *Ann. Geophys.*, *19*, 1, 1963.

Behannon, K. W., F. M. Neubauer, and H. Barnstorf, Finescale characteristics of interplanetary sector boundaries, *J. Geophys. Res.*, *86*, 3273, 1981.

Bird, M. K., and P. Edenhofer, Remote sensing observations of the solar corona, in *Physics of the Inner Heliosphere*, vol. 1, *Large-Scale Phenomena*, edited by R. Schwenn and E. Marsch, p. 13, Springer-Verlag, New York, 1990.

Bothmer, V., and R. Schwenn, Eruptive prominences as sources of magnetic clouds in the solar wind, *Space Sci. Rev.*, *70*, 215, 1994.

Bravo, S., B. Mendoza, and R. Perez-Enriquez, Coronal holes as sources of large-scale solar wind disturbances and geomagnetic perturbations, *J. Geophys. Res.*, *96*, 5387, 1991.

Burlaga, L. F. E., Magnetic clouds, in *Physics of the Inner Heliosphere*, vol. 2, *Particles, Waves and Turbulence*, edited by R. Schwenn and E. Marsch, p. 1, Springer-Verlag, New York, 1991.

Burlaga, L. F., and J. H. King, Intense interplanetary magnetic fields observed by geocentric spacecraft during 1963–1975, *J. Geophys. Res.*, *84*, 6633, 1979.

Burlaga, L. F., K. W. Behannon, and L. W. Klein, Compound streams, magnetic clouds, and major geomagnetic storms, *J. Geophys. Res.*, *92*, 5725, 1987.

Cane, H. V., and D. V. Reames, Some statistics of solar radio bursts of spectral types II and IV, *Astrophys. J.*, *325*, 901, 1988.

Cane, H. V., S. W. Kahler, and N. R. Sheeley, Jr., Interplanetary shocks preceded by solar filament eruptions, *J. Geophys. Res.*, *91*, 13,321, 1986.

Chapman, S., Historical introduction to aurora and magnetic storms, *Ann. Geophys.*, *24*, 497, 1968.

Chapman, S., and J. Bartels, *Geomagnetism*, chap. 12, p. 5, Clarendon Press, Oxford, England, 1940.

Cliffswallow, W. (Ed.), Region 5395 of March 1989, *NOAA Tech. Memo. ERL SEL-82*, Space Environ. Lab., Boulder, Colo., 1993.

Cliver, E. W., and N. U. Crooker, A seasonal dependence for the geoeffectiveness of eruptive solar events, *Sol. Phys.*, *145*, 347, 1993.

Clúa de Gonzalez, A. L., W. D. Gonzalez, S. L. G. Dutra, and B. T. Tsurutani, Periodic variation in the geomagnetic activity: A study based on the *Ap* index, *J. Geophys. Res.*, *98*, 9215, 1993.

Crooker, N. U., and E. W. Cliver, Postmodern view of *M*-regions, *J. Geophys. Res.*, *99*, 23,383, 1994.

Crooker, N. U., E. W. Cliver, and B. T. Tsurutani, The semiannual variation of great geomagnetic storms and the postshock Russell-McPherron effect preceding coronal mass ejecta, *Geophys. Res. Lett.*, *19*, 429, 1992.

Crooker, N. U., G. L. Siscoe, S. Shodhan, D. F. Webb, J. T. Gosling, and E. J. Smith, Multiple heliospheric current sheets and coronal streamer belt dynamics, *J. Geophys. Res.*, *98*, 9371, 1993.

Dodson, H. W., and E. R. Hedeman, Comments on filament-disintegration and its relation to other aspects of solar activity, *Sol. Phys.*, *23*, 360, 1972.

Dodson, H. W., E. R. Hedeman, and O. C. Mohler, Examples of "problem" flares or situations in past solar-terrestrial observations, in *Proceedings of the 1979 Solar-Terrestrial Predictions Workshop*, p. 385, Natl. Oceanic and Atmos. Admin., Boulder, Colo., 1979.

Erskine, F. T., W. M. Cronyn, S. D. Shawhan, E. C. Roelof, and B. L. Gotwols, Interplanetary scintillation at large elongation angles: Response to solar wind density structure, *J. Geophys. Res.*, *83*, 4153, 1978.

Feldman, W. C., J. R. Asbridge, S. J. Bame, E. E. Fenimore, and J. T. Gosling, The solar origins of solar wind interstream flows: Near-equatorial coronal streamers, *J. Geophys. Res.*, *86*, 5408, 1981.

Feynman, J., Geomagnetic and solar wind cycles, 1900–1975, *J. Geophys. Res.*, *87*, 6153, 1982.

Feynman, J., and N. U. Crooker, The solar wind at the turn of the century, *Nature*, *275*, 626, 1978.

Feynman, J., and P. F. Fougere, Eighty-eight year periodicity in solar-terrestrial phenomena confirmed, *J. Geophys. Res.*, *89*, 3023, 1984.

Feynman, J., and X. Y. Gu, Prediction of geomagnetic activity on time scales of one to ten years, *Rev. Geophys.*, *24*, 650, 1986.

Feynman, J., and S. M. Silverman, Auroral changes during the eighteenth and nineteenth centuries and their implications for the solar wind and the long-term variation of sunspot activity, *J. Geophys. Res.*, *85*, 2991, 1980.

Fraser-Smith, A. C., Spectrum of the geomagnetic index Ap, J. Geophys. Res., *77*, 4209, 1972.

Freeman, J., A. Nagai, P. Reiff, W. Denig, S. Gussenhoven, M. A. Shea, M. Heinemann, F. Rich, and M. Hairston, The use of neural networks to predict magnetospheric parameters for input to a magnetospheric forecast model, in *Proceedings of the 1993 International Workshop on Artificial Intelligence Applications in Solar-Terrestrial Physics*, p. 167, Natl. Oceanic and Atmos. Admin., NOAA, Boulder, Colo., 1993.

Gonzalez, A. L. C., and W. D. Gonzalez, Periodicities in the interplanetary magnetic field polarity, *J. Geophys. Res.*, *92*, 4357, 1987.

Gonzalez, W. D., and B. T. Tsurutani, Criteria of interplanetary parameters causing intense magnetic storm ($Dst < -100$ nT), *Planet. Space Sci.*, *35*, 1101, 1987.

Gonzalez, W. D., J. A. Joselyn, Y. Kamide, H. W. Kroehl, G. Rostoker, B. T. Tsurutani, and V. M. Vasyliunas, What is a geomagnetic storm?, *J. Geophys. Res.*, *99*, 5771, 1994.

Gosling, J. T., Coronal mass ejections and magnetic flux ropes in interplanetary space, in *Physics of Magnetic*

Flux Ropes, *Geophys. Monogr. Ser.*, vol. 58, C. T. Russell, E. R. Priest, and L. C. Lee, p. 343, AGU, Washington, D. C., 1990.
Gosling, J. T., The solar flare myth, *J. Geophys. Res.*, *98*, 18937, 1993.
Gosling, J. T., and D. J. McComas, Field line draping about fast coronal mass ejecta: A source of strong out-of-the ecliptic interplanetary magnetic fields, *Geophys. Res. Lett.*, *14*, 355, 1987.
Gosling, J. T., E. Hildner, J. R. Asbridge, S. J. Bame, and W. C. Feldman, Noncompressive density enhancements in the solar wind, *J. Geophys. Res.*, *82*, 5005, 1977.
Gosling, J. T., D. N. Baker, S. J. Bame, W. C. Feldman, R. D. Zwickl, and E. J. Smith, Bidirectional solar wind electron heat flux events, *J. Geophys. Res.*, *92*, 8519, 1987.
Gosling, J. T., S. J. Bame, D. J. McComas, and J. L. Phillips, Coronal mass ejections and large geomagnetic storms, *Geophys. Res. Lett.*, *17*, 901, 1990.
Gosling, J. T., D. J. McComas, J. L. Phillips, and S. J. Bame, Geomagnetic activity associated with Earth passage of interplanetary shock disturbances and coronal mass ejections, *J. Geophys. Res.*, *96*, 7831, 1991.
Green, C. A., The semiannual variation in the magnetic activity indices *aa* and *Ap*, *Planet. Space Sci.*, *32*, 297, 1984.
Hapgood, M. A., A double solar cycle in the 27-day recurrence of geomagnetic activity, *Ann. Geophys.*, *11*, 248, 1993.
Hedin, A. E., MSIS-86 thermospheric model, *J. Geophys. Res.*, *92*, 4649, 1987.
Hirshburg, J., and D. S. Colburn, Geomagnetic activity at sector boundaries, *J. Geophys. Res.*, *78*, 3952, 1973.
Hoeksema, J. T., Solar sources of geomagnetic storms, *Eos Trans. AGU*, *73*(3), 34, 1992.
Hoeksema, J. T., Coronal and interplanetary magnetic field topology, in *Proceedings of the 1992 Solar-Terrestrial Predictions Workshop*, vol. 2, p. 3, Natl. Oceanic and Atmos. Admin., Boulder, Colo., 1993.
Hoeksema, J. T., and X. Zhao, Prediction of magnetic orientation in driver gas associated $-B_z$ events, *J. Geophys. Res.*, *97*, 3151, 1992.
Hoeksema, J. T., J. M. Wilcox, and P. H. Scherrer, Structure of the heliospheric current sheet in the early portion of sunspot cycle 21, *J. Geophys. Res.*, *87*, 10,331, 1982.
Hundhausen, A. J., An interplanetary view of coronal holes, in *Coronal Holes and High Speed Solar Wind Streams*, edited by J. B. Zirker, p. 225, Colo. Assoc. Univ. Press, Boulder, 1977.
Hundhausen, A. J., The size and locations of coronal mass ejections: SMM observations from 1980 and 1984–1989, *J. Geophys. Res.*, *98*, 13,177, 1993.
Jackson, B. V., and C. Leinert, Helios images of solar mass ejections, *J. Geophys. Res.*, *90*, 10,759, 1985.
Jackson, B. V., G. A. Dulk, and K. V. Sheridan, in *Solar and Interplanetary Dynamics*, edited by M. Dryer and E. Tandberg-Hanssen, p. 379, D. Reidel, Norwell, Mass., 1980.
Jackson, B., R. Gold, and R. Altrock, The solar mass ejection imager, *Adv. Space Res.*, *11*(1), 377, 1991.
Jacobs, J. A., *Reversals of the Earth's Magnetic Field*, Adam Hilger, Bristol, England, 1984.
Joselyn, J. A., SESC methods for short-term geomagnetic predictions in *Proceedings of the 1984 Solar-Terrestrial Predictions Workshop*, p. 404, Natl. Oceanic and Atmos. Admin., Boulder, Colo., 1986a.
Joselyn, J. A., Real-time prediction of global geomagnetic activity, in *Solar Wind–Magnetosphere Coupling*, edited by Y. Kamide and J. A. Slavin, 127, Terra Sci. Tokyo, 1986b.
Joselyn, J. A., Geomagnetic quiet day selections, *Pure Appl. Geophys.*, *131*, 333, 1989.
Joselyn, J. A., Forecasting magnetically quiet periods, in *Proceedings of the 1989 Solar-Terrestrial Predictions Workshop*, vol. 1., p. 102, Natl. Oceanic and Atmos. Admin., Boulder, Colo., 1990.
Joselyn, J. A., and P. S. McIntosh, Disappearing solar filaments: A useful predictor of geomagnetic activity, *J. Geophys. Res.*, *86*, 4555, 1981.
Joselyn, J. A., and B. T. Tsurutani, Geomagnetic sudden impulses and storm sudden commencements, *Eos Trans. AGU*, *71*, 1808, 1990.
Joselyn, J. A., J. Hirman, and G. R. Heckman, ISEE 3 in real time, *Eos Trans. AGU*, *62*, 617, 1981.
Joselyn, J. A., J. A. Flueck, and T. Brown, Geomagnetic climatology, *Ann. Geophys.*, *6*, 595, 1988.
Kahler, S. W., Solar flares and coronal mass ejections, *Annu. Rev. Astron. Astrophys.*, *30*, 113, 1992.
Kahler, S., A search for geomagnetic storm evidence of the reversal of the solar dipole magnetic field and interplanetary B_z, *J. Geophys. Res.*, *98*, 3485, 1993a.
Kahler, S. W., Coronal mass ejections and long rise times of solar energetic particle events, *J. Geophys. Res.*, *98*, 5607, 1993b.
Kahler, S. W., E. Hildner, and M. A. I. Van Hollebeke, Prompt solar proton events and coronal mass ejections, *Sol. Phys.*, *57*, 429, 1978.
Kahler, S. W., N. R. Sheeley Jr., R. A. Howard, M. J. Koomen, D. J. Michels, R. E. McGuire, T. T. von Rosenvinge, and D. V. Reames, Associations between coronal mass ejections and solar energetic proton events, *J. Geophys. Res.*, *89*, 9683, 1984.
Klein, L. W., and L. F. Burlaga, Interplanetary magnetic clouds at 1 AU, *J. Geophys. Res.*, *87*, 613, 1982.
Lanzerotti, L. J. (Ed.), Impacts of ionospheric/magnetospheric processes on terrestrial science and technology, in *Solar System Plasma Physics*, vol. III, edited by L. J. Lanzerotti, C. F. Kennel, and E. N. Parker, p. 317, North-Holland, New York, 1979.
Lanzerotti, L. J., C. G. Maclennan, and A. C. Fraser-Smith, Background magnetic spectra: 10^{-5} to 10^5 Hz, *Geophys. Res. Lett.*, *17*, 1593, 1990.
Legrand, J.-P., and P. A. Simon, Ten cycles of solar and geomagnetic activity, *Sol. Phys.*, *70*, 173, 1981.
Legrand, J.-P., and P. A. Simon, A two-component solar cycle, *Sol. Phys.*, *131*, 187, 1991.
Leinbach, H., S. Ananthakrishnan, and T. R. Detman, The utility of interplanetary scintillation maps in forecasting geomagnetic activity: A study based on single-station data from Cambridge, United Kingdom, *NOAA Tech. Memo. ERL SEL-83*, Space Environ. Lab., Boulder, Colo., 1994.
Lincoln, J. V., Geomagnetic indices, in *Physics of Geomagnetic Phenomena*, vol. 1, edited by S. Matsushita and W. H. Campbell, p. 67, Academic, San Diego, Calif., 1967.
Lundstedt, H., P. H. Scherrer, and J. M. Wilcox, Geomagnetic activity and Hale sector boundaries, *Planet. Space Sci.*, *29*, 167, 1981.
Marsden, R. G., T. R. Sanderson, C. Tranquille, K.-P. Wenzel, and E. J. Smith, ISEE 3 observations of low-energy proton bidirectional events and their relation to isolated interplanetary magnetic structures, *J. Geophys. Res.*, *92*, 11,009, 1987.
Marubashi, K., Structure of the interplanetary magnetic clouds and their solar origins, *Adv. Space Res.*, *6*, 335, 1986.
Matsushita, S., Solar quiet and lunar daily variation fields, in

Physics of Geomagnetic Phenomena, vol. 1, edited by S. Matsushita and W. H. Campbell, p. 302, Academic, San Diego, Calif., 1967.

Mayaud, P. N. (Ed.), *Derivation, Meaning, and Use of Geomagnetic Indices*, *Geophys. Monogr. Ser.*, vol. 22, AGU, Washington, D. C., 1980.

McComas, D. J., J. T. Gosling, S. J. Bame, E. J. Smith, and H. V. Cane, A test of magnetic field draping induced B_z perturbations ahead of fast coronal mass ejecta, *J. Geophys. Res.*, *94*, 1465, 1989.

McIntosh, P. S., Solar magnetic fields derived from hydrogen-alpha filtergrams, *Rev. Geophys.*, *10*, 837, 1972.

McNamara, L. F., and C. S. Wright, Disappearing solar filaments and geomagnetic activity, *Nature*, *299*, 537, 1982.

McPherron, R. L., Possible applications of expert systems and fuzzy logic in solar terrestrial physics, in *Proceedings of the International Workshop on Artificial Intelligence Applications in Solar-Terrestrial Physics*, p. 1, Natl. Oceanic and Atmos. Admin., Boulder, Colo., 1993.

Menvielle, M., and A. Berthelier, The *K*-derived planetary indices: Description and availability, *Rev. Geophys.*, *29*, 415, 1991. (Correction, *Rev. Geophys.*, *30*, 91, 1992.)

Menvielle, M., and A. Berthelier, Correction to The *K*-derived planetary indices: Description and availability, *Rev. Geophys.*, *30*, 91, 1992.

Moore, V., and R. A. Harrison, A characterization of discrete solar wind events detected by interplanetary scintillation mapping, *J. Geophys. Res.*, *99*, 27, 1994.

Munro, R. H., J. T. Gosling, E. Hildner, R. M. MacQueen, A. I. Poland, and C. L. Ross, The association of coronal mass ejection transients with other forms of solar activity, *Sol. Phys.*, *61*, 201, 1979.

Neugebauer, M., Observational constraints on solar wind acceleration mechanisms, in Solar Wind Five, edited by M. Neugebauer, *NASA Conf. Publ.*, *cp2280*, 135, 1983.

Neugebauer, M., The problem of associating solar and interplanetary events, in Solar Wind Six, edited by V. Pizzo, T. Holzer, and D. Sime, vol. 1, *Tech. Note NCAR/TN-306+ Proc.*, p. 243, Natl. Cent. for Atmos. Res., Boulder, Colo., 1988.

Neupert, W. M., and V. Pizzo, Solar coronal holes as sources of recurrent geomagnetic disturbances, *J. Geophys. Res.*, *79*, 3701, 1974.

Nolte, J. T., A. S. Krieger, A. F. Timothy, R. E. Gold, E. C. Roelof, G. Vaiana, A. J. Lazarus, J. D. Sullivan, and P. S. McIntosh, Coronal holes as sources of solar wind, *Sol. Phys.*, *46*, 303, 1976.

Perez-Enriquez, R., and B. Mendoza, Geomagnetic response of the Earth to crossings of the heliospheric current sheet, *J. Geophys. Res.*, *98*, 19,349, 1993.

Phillips, J. L., J. T. Gosling, and D. J. McComas, Coronal mass ejections and geomagnetic storms: Seasonal variations, in *Proceedings of the 1992 Solar-Terrestrial Predictions Workshop*, vol. 3, p. 242, Natl. Oceanic and Atmos. Admin., Boulder, Colo., 1993.

Pudovkin, M. I., and A. D. Chertkov, The magnetic field of the solar wind, *Sol. Phys.*, *50*, 213, 1976.

Reames, D. V., Recent observations and the modeling of solar proton events, in *Proceedings of the 1992 Solar-Terrestrial Predictions Workshop*, vol. 2, p. 302, Natl. Oceanic and Atmos. Admin., Boulder, Colo., 1993.

Richardson, I. G., and H. V. Cane, Signatures of shock drivers in the solar wind and their dependence on the solar source location, *J. Geophys. Res.*, *98*, 15,295, 1993.

Richardson, I. G., C. J. Farrugia, and D. Winterhalter, Solar activity and coronal mass ejections on the western hemisphere of the Sun in mid-August 1989: Association with interplanetary observations at the ICE and IMP 8 spacecraft, *J. Geophys. Res.*, *99*, 2513, 1994.

Rostoker, G., Geomagnetic indices, *Rev. Geophys.*, *10*, 935, 1972.

Rostoker, G., S.-I. Akasofu, W. Baumjohann, Y. Kamide, and R. L. McPherron, The roles of direct input of energy from the solar wind and unloading of stored magnetotail energy in driving magnetospheric substorms, *Space Sci. Rev.*, *46*, 93, 1987.

Russell, C. T., and R. L. McPherron, Semiannual variation of geomagnetic activity, *J. Geophys. Res.*, *78*, 92, 1973.

Russell, C. T., R. L. McPherron, and R. E. Burton, On the cause of geomagnetic storms, *J. Geophys. Res.*, *79*, 1105, 1974.

Sanchez-Ibarra, A., and M. Barraza-Paredes, Catalogue of Coronal Holes 1970–1991, *Rep. UAG-102*, World Data Cent. A for Sol.-Terr. Phys., Natl. Geophys. Data Cent., Boulder, Colo., 1992.

Sargent, H. H., III, The 27-day recurrence index, in *Solar Wind-Magnetosphere Coupling*, edited by Y. Kamide and J. A. Slavin, p. 143, Terra Sci., Tokyo, 1986.

Schwenn, R., Direct correlation between coronal transients and interplanetary disturbances, *Space Sci. Rev.*, *34*, 85, 1983.

Schwenn, R., Relationship of coronal transients to interplanetary shocks: 3D aspects, *Space Sci. Rev.*, *44*, 139, 1986.

Schwenn, R., Large-scale structures of the interplanetary medium, in *Physics of the Inner Heliosphere I*, edited by R. Schwenn and E. Marsch, p. 99, Springer-Verlag, New York, 1990.

Sheeley, N. R., Jr., and J. W. Harvey, Coronal holes, solar wind streams, and geomagnetic disturbances during 1978 and 1979, *Sol. Phys.*, *70*, 237, 1981.

Sheeley, N. R., Jr., et al., Coronal changes associated with a disappearing filament, *Sol. Phys.*, *45*, 377, 1975.

Sheeley, N. R., Jr., R. A. Howard, M. J. Koomen, and D. J. Michels, Associations between coronal mass ejections and soft x-ray events, *Astrophys. J.*, *272*, 349, 1983.

Sheeley, N. R., Jr., R. T. Stewart, R. D. Robinson, R. A. Howard, M. J. Koomen, and D. J. Michels, Associations between coronal mass ejections and metric type II bursts, *Astrophys. J.*, *279*, 839, 1984.

Sheeley, N. R., Jr., R. A. Howard, M. J. Koomen, D. J. Michels, R. Schwenn, K. H. Muhlhauser, and H. Rosenbauer, Coronal mass ejections and interplanetary shocks, *J. Geophys. Res.*, *90*, 163, 1985.

Tang, F., S.-I. Akasofu, E. Smith, and B. Tsurutani, Magnetic fields on the Sun and the north-south component of transient variations of the interplanetary magnetic field at 1 AU, *J. Geophys. Res.*, *90*, 2703, 1985.

Tang, F., B. T. Tsurutani, W. D. Gonzalez, S.-I. Akasofu, and E. J. Smith, Solar sources of interplanetary southward B_z events responsible for major magnetic storms (1978–1979), *J. Geophys. Res.*, *94*, 3535, 1989.

Thompson, R., G. Heckman, and J. Hirman, The world space weather service, in *Proceedings of the 1992 Solar-Terrestrial Predictions Workshop*, vol. 1, p. 17, Natl. Oceanic and Atmos. Admin., Boulder, Colo., 1993.

Thomson, A. W. P., Neural networks and non-linear prediction of geomagnetic activity, in *Proceedings of the 1993 International Workshop on Artificial Intelligence Applications in Solar-Terrestrial Physics*, p. 133, Natl. Oceanic and Atmos. Admin., NOAA, Boulder, Colo., 1993.

Thomson, A. W. P., T. D. G. Clark, and D. J. Kerridge, Forecasting *Ap* in the short-term using time series analysis, in *Proceedings of the 1992 Solar-Terrestrial Predictions Workshop*, vol. 3, p. 269, Natl. Oceanic and Atmos. Admin., NOAA, Boulder, Colo., 1993.

Tsurutani, B. T., W. D. Gonzalez, F. Tang, S.-I. Akasofu, and E. J. Smith, Origin of interplanetary southward magnetic fields responsible for major magnetic storms near solar maximum (1978–1979), *J. Geophys. Res.*, *93*, 8519, 1988.

Wang, Y.-M., and N. R. Sheeley Jr., The solar origin of long-term variations of the interplanetary magnetic field strength, *J. Geophys. Res.*, *93*, 11,227, 1988.

Wang, Y.-M., and N. R. Sheeley Jr., Solar wind speed and coronal flux-tube expansion, *Astrophys. J.*, *355*, 726, 1990.

Watanabe, T., and R. Schwenn, Large-scale propagation properties of interplanetary disturbances revealed from IPS and spacecraft observations, *Space Sci. Rev.*, *51*, 147, 1989.

Watari, S., The latitudinal distribution of coronal holes and geomagnetic storms due to coronal holes, in *Proceedings of the 1989 Solar-Terrestrial Predictions Workshop*, vol. 1, p. 627, Natl. Oceanic and Atmos. Admin., NOAA, Boulder, Colo., 1990.

Webb, D. F., The heliospheric manifestation and geoeffectiveness of solar mass ejections, in *Proceedings of the 1992 Solar-Terrestrial Predictions Workshop*, vol. 2, p. 71, Natl. Oceanic and Atmos. Admin., Boulder, Colo., 1993.

Webb, D. F., and A. J. Hundhausen, Activity associated with the solar origin of coronal mass ejections, *Sol. Phys.*, *108*, 383, 1987.

Wilcox, J. M., and N. F. Ness, Quasi-stationary corotating structure in the interplanetary medium, *J. Geophys. Res.*, *70*, 5793, 1965.

Wilson, L., An evaluation of digitally derived *K*-indices, *J. Geomagn. Geoelectr.*, *39*, 97, 1987.

Wilson, R. M., Geomagnetic response to magnetic clouds, *Planet. Space Sci.*, *35*, 329, 1987.

Wilson, R. M., On the behavior of the *Dst* geomagnetic index in the vicinity of magnetic cloud passages at Earth, *J. Geophys. Res.*, *95*, 215, 1990.

Wilson, R. M., and E. Hildner, Are interplanetary magnetic clouds manifestations of coronal transients at 1 AU?, *Sol. Phys.*, *91*, 169, 1984.

Wilson, R. M., and E. Hildner, On the association of magnetic clouds with disappearing filaments, *J. Geophys. Res.*, *91*, 5867, 1986.

Woo, R., Solar cycle variation of interplanetary disturbances observed as Doppler scintillation transients, *J. Geophys. Res.*, *98*, 18,999, 1993.

Woo, R., and P. Gazis, Large-scale solar-wind structure near the Sun detected by Doppler scintillation, *Nature*, *366*, 543, 1993.

Woo, R., and R. Schwenn, Comparison of Doppler scintillation and in situ spacecraft plasma measurements of interplanetary disturbances, *J. Geophys. Res.*, *96*, 21,227, 1991.

Woo, R., J. W. Armstrong, N. R. Sheeley, Jr., R. A. Howard, M. J. Koomen, D. J. Michels, and R. Schwenn, Doppler scintillation observations of interplanetary shocks within 0.3 AU, *J. Geophys. Res.*, *90*, 154, 1985.

Wright, C. S., Disappearing filaments and geomagnetic storms—The role of filament orientation, in *Proceedings of the 1984 Solar-Terrestrial Predictions Workshop*, p. 420, Natl. Oceanic and Atmos. Admin., Boulder, Colo., 1986.

Wright, C. S., and L. F. McNamara, The relationships between disappearing solar filaments, coronal mass ejections, and geomagnetic activity, *Sol. Phys.*, *87*, 401, 1983.

Wright, C. S., and D. F. Webb, The signatures of disappearing filaments in the interplanetary medium at 1 AU, in *Proceedings of the 1989 Solar-Terrestrial Predictions Workshop*, vol. 1, p. 664, Natl. Oceanic and Atmos. Admin., Boulder, Colo., 1990.

Zhang, G., and L. F. Burlaga, Magnetic clouds, geomagnetic disturbances, and cosmic ray decreases, *J. Geophys. Res.*, *93*, 2511, 1988.

J. A. Joselyn, NOAA Space Environment Laboratory, 325 Broadway, Boulder, CO 80303. (e-mail: jjoselyn@sel.noaa.gov)